The EMBO Journal (2012) 31, 2615–2628 | © 2012 European Molecular Biology Organization | All Rights Reserved 0261-4189/12
www.embojournal.org

THE EMBO JOURNAL

Caspase-2 is an initiator caspase responsible for pore-forming toxin-mediated apoptosis

Gergely Imre[1], Jan Heering[2], Armelle-Natsuo Takeda[1], Matthias Husmann[3], Bernd Thiede[4], Dagmar Meyer zu Heringdorf[5], Douglas R Green[6], F Gisou van der Goot[7], Bhanu Sinha[8,9], Volker Dötsch[2] and Krishnaraj Rajalingam[1,*]

[1]Emmy Noether Group of the DFG, Institute of Biochemistry II, Goethe University, Frankfurt, Germany, [2]Institute of Biophysical Chemistry and Center for Biomolecular Magnetic Resonance, Goethe University, Frankfurt, Germany, [3]Institute of Medical Microbiology and Hygiene, University Medical Center, Johannes Gutenberg-University Mainz, Hochhaus am Augustusplatz, Mainz, Germany, [4]The Biotechnology Centre of Oslo, University of Oslo, Oslo, Norway, [5]Pharma Zentrum, Goethe University Medical School, Frankfurt, Germany, [6]Department of Immunology, St Jude Children's Research Hospital, Memphis, Tennessee, USA, [7]Faculty of Life Sciences, The Global Health Institute, Ecole Polytechnique Fédérale de Lausanne, Lausanne, Switzerland and [8]Department of Medical Microbiology, University of Groningen, University Medical Center Groningen, Groningen, The Netherlands

Bacterial pathogens modulate host cell apoptosis to establish a successful infection. Pore-forming toxins (PFTs) secreted by pathogenic bacteria are major virulence factors and have been shown to induce various forms of cell death in infected cells. Here we demonstrate that the highly conserved caspase-2 is required for PFT-mediated apoptosis. Despite being the second mammalian caspase to be identified, the role of caspase-2 during apoptosis remains enigmatic. We show that caspase-2 functions as an initiator caspase during *Staphylococcus aureus* α-toxin- and *Aeromonas* aerolysin-mediated apoptosis in epithelial cells. Downregulation of caspase-2 leads to a strong inhibition of PFT-mediated apoptosis. Activation of caspase-2 is PIDDosome-independent, and endogenous caspase-2 is recruited to a high-molecular-weight complex in α-toxin-treated cells. Interestingly, prevention of PFT-induced potassium efflux inhibits the formation of caspase-2 complex, leading to its inactivation, thus resisting apoptosis. These results revealed a thus far unknown, obligatory role for caspase-2 as an initiator caspase during PFT-mediated apoptosis.

The EMBO Journal (2012) **31,** 2615–2628. doi:10.1038/emboj.2012.93; Published online 24 April 2012
Subject Categories: signal transduction; differentiation & death
Keywords: apoptosis; caspase; caspase-2; pore-forming toxin; staphylococcus

*Corresponding author. Emmy Noether Group of the DFG, Institute of Biochemistry II, Goethe University Medical School, Frankfurt 60590, Germany. Tel.: +49 69 6301 5450; Fax: +49 6963015577;
E-mail: Krishna@biochem2.de
[9]Previous address: Institute for Hygiene and Microbiology, University of Würzburg, Würzburg, Germany

Received: 14 February 2012; accepted: 8 March 2012; published online 24 April 2012

Introduction

Apoptosis is a form of programmed cell death primarily characterized by the presence of unique morphological and biochemical features (Kroemer *et al*, 2009). Apoptosis is initiated by two major pathways, namely extrinsic or receptor-mediated and intrinsic or mitochondria-mediated pathways (Meier and Vousden, 2007). One of the features of apoptotic cell death is the activation of caspases, a class of cysteine proteases. Depending on the structure and chronology of activation, caspases are primarily classified into initiator and effector caspases (Thornberry and Lazebnik, 1998). Caspases-8 and -9 are recognized as initiator caspases, and caspases-3, -6 and -7 are recognized as effector caspases (Shi, 2004). Intriguingly, caspase-2 exhibits feature of both initiator and effector caspases (Troy and Shelanski, 2003). The unique apoptotic modalities, where caspase-2 functions as an initiator caspase, however remain unclear (Krumschnabel *et al*, 2009).

Pathogens have acquired elaborate strategies to modulate host cell death to establish successful infection and propagation (Lamkanfi and Dixit, 2010; Rudel *et al*, 2010). Pore-forming toxins (PFTs) are one of the major classes of bacterial toxins (~25% of all protein toxins) secreted by pathogenic bacteria to elicit membrane injury on host cells (Bischofberger *et al*, 2009). Upon toxin-mediated membrane damage, the cells usually respond by triggering various signalling pathways that could lead to the activation of inflammasomes, membrane recovery, quiescence and autophagy (Abrami *et al*, 2000; Gonzalez *et al*, 2011). However, persistent membrane damage by PFTs often leads to cell death, which could be apoptosis, necrosis, or pyroptosis depending on the concentration of the toxins and cell types (Walev *et al*, 1993; Warny and Kelly, 1999; Bantel *et al*, 2001; Haslinger *et al*, 2003; Genestier *et al*, 2005; Saleh and Green, 2007; Craven *et al*, 2009; Srivastava *et al*, 2009). The α-hemolysin (α-toxin) secreted by human pathogen *Staphylococcus aureus* is a classical PFT, which has been shown to induce caspase-1-mediated pyroptosis in macrophages and caspase-dependent apoptotic cell death in lymphocytes (Warny and Kelly, 1999; Bantel *et al*, 2001; Haslinger *et al*, 2003; Fernandes-Alnemri *et al*, 2007; Craven *et al*, 2009). The Gram-positive pathogen *S. aureus* can cause a broad spectrum of pathological conditions such as pneumonia, osteomyelitis, endocarditis, blood stream infections, toxic shock syndromes and other toxin-mediated diseases. One major virulence factor of *S. aureus* is α-toxin, secreted as a 33.3 kDa water-soluble monomer. Upon binding to cells it undergoes oligomerization to form heptameric pores of 1–2 nm in size in the host cell plasma membrane (Iacovache *et al*, 2010). Recent studies revealed ADAM10 as a potential proteinaceous high-affinity receptor for α-toxin in host cells (Wilke and Bubeck, 2010), whereas phosphatidylcholine heads have been reported to serve as low-affinity receptors (Galdiero and Gouaux, 2004).

Aerolysin is another PFT secreted by a human enteropathogen, *Aeromonas hydrophila*. Aerolysin is secreted as an inactive precursor (Abrami *et al*, 2000, 2003). Upon binding to host cell surface, pro-aerolysin undergoes processing into aerolysin, which, as α-toxin, forms heptameric pores to elicit membrane injury and cell death (Abrami *et al*, 2003). Despite intense efforts, the molecular machinery driving PFTs-mediated host cell death remains poorly understood. Here we unveil a unique role for caspase-2 during PFT-mediated apoptosis in epithelial cells and fibroblasts. Initiator caspases are normally activated by dimerization when brought into close proximity by adaptor proteins in multimeric protein complexes (Mace and Riedl, 2010). In response to death receptors, caspase-8 is activated in a multimeric protein complex, named DISC, whereas caspase-9 is activated by the assembly of a multimeric protein complex, named the apoptosome, which is triggered by the release of cytochrome *c* from mitochondria (Mace and Riedl, 2010). Previously, caspase-2 has been shown to be recruited to a $\geq$600-kDa protein complex, named PIDDosome, which contains PIDD (p53-induced protein with a death domain DD) and RAIDD (adaptor protein RAIDD, receptor-interacting protein-associated ICH-1/CED-3 homologous protein with a DD) (Tinel and Tschopp, 2004). Here we found that activation of caspase-2 is independent of the PIDDosome, and endogenous caspase-2 is recruited to a novel high-molecular-weight (HMW) complex in PFT-treated cells. Interestingly, recruitment of caspase-2 to this HMW complex and activation are dependent on PFT-mediated K^+ efflux. We further demonstrate that PFT-mediated cell death is dependent on mitochondrial outermembrane permeabilization (MOMP) and effector caspases downstream of caspase-2. This study unveils the molecular machinery driving PFT-mediated cytotoxicity in epithelial cells and in addition, sheds further light onto the mechanisms behind activation of caspase-2, a highly conserved caspase during host–pathogen interaction.

Results

S. aureus α-toxin induced caspase-dependent apoptosis in epithelial cells

As epithelia are the prime site of many infections, we set out to explore the molecular mechanisms behind α-toxin-mediated apoptosis in epithelial cells.

Treatment of HeLa cells with purified *S. aureus* α-toxin from two different preparations led to apoptotic cell death in a concentration- and time-dependent manner, as measured by two different assays (Figure 1A and Supplementary Figure S1A–D). Similar results were obtained when the cells were treated with virulent bacterial culture supernatants (Figure 1B and Supplementary Figure S1E and F). Compared to mononuclear leucocytes, HeLa cells were at least 10-fold less susceptible for cell death induction. As α-toxin has been shown to induce non-apoptotic forms of cell death in macrophages and lymphocytes, we initially characterized the mode of cell death elicited by this toxin in HeLa cells by using two different assays to measure apoptotic cell death. Treatment with *S. aureus* α-toxin led to the exposure of phosphatidylserine in HeLa cells as early as 6 h after treatment, as revealed by an increase in annexin-V-positive cells (Supplementary Figure S1C). At later time points (12–24 h), the annexin-V single-positive cells became annexin-V–PI double positive, accompanied by DNA fragmentation (Supplementary Figure S1C and D). These results support the notion that the membrane integrity loss is a post-apoptotic, secondary event during α-toxin-mediated apoptosis. The cell death observed with either bacterial culture supernatants or with purified α-toxin can be fully rescued by co-incubation with α-toxin antibody (Supplementary Figure S2A, and data not shown). *S. aureus* α-toxin elicits its cytotoxic response by the assembly of heptameric β-barrel pores on the host cell plasma membrane. We checked if pore formation is required for mediating cell death by this toxin. As predicted, a pore-dead single amino-acid exchange mutant of α-toxin (D152C) failed to induce apoptosis in these cell types (Supplementary Figure S2B). We then tested if cell death induced by α-toxin is dependent on the activation of caspases. As predicted, pre-treatment of cells with broad spectrum caspase inhibitor zVAD–fmk largely prevented α-toxin or bacterial supernatant-mediated apoptosis, as measured by three different assays (Figure 1C–F and Supplementary Figure S2C). To check if treatment of HeLa cells with α-toxin leads to mitochondrial changes observed during apoptosis, we checked for the loss of mitochondrial membrane potential (MMP) and release of proapoptogenic factors like Smac/Diablo from the mitochondria. As expected, PFT treatment has led to a caspase-dependent loss of MMP in HeLa cells (Supplementary Figure S3A). Further, significant Smac/Diablo levels are found in the cytosol of α-toxin-treated cells with no significant alterations in Bid levels (Supplementary Figure S3B and C). Induction of apoptosis is not confined to HeLa cells alone, as α-toxin can also induce caspase-dependent cell death in early passage primary epithelial cells derived from human trachea (Supplementary Figure S4A). To uncover the spectrum of activated caspases, we prepared cell lysates from α-toxin-treated HeLa cells and probed them with antibodies directed against various caspases. Interestingly, we detected the processing of caspases-8, -9, -2, -3 and the well-studied caspase substrate PARP in α-toxin-treated cells (Figure 1F). While caspases-8, -9 and -3 activation in response to α-toxin has been detected before in other cell types such as leukocytes (Bantel *et al*, 2001; Haslinger *et al*, 2003), the processing of caspase-2 upon toxin treatment has not been reported. The degradation of caspase-8 even in the presence of caspase inhibitor might be due to the fact that at later time points the whole proteome degrades owing to complete cell lysis. Interestingly, processing of caspase-2 was also detected in other cell types including human primary epithelial cells and freshly isolated human foreskin keratinocytes after PFT treatment, suggesting that the observed effect is not confined to HeLa cells (Supplementary Figure S4B and C). These results revealed that caspases are processed and are required during PFT-mediated apoptosis in multiple cell types.

Caspase-2 functions as an initiator caspase during PFT-mediated apoptosis

As caspase-2 exhibits feature of both initiator and effector caspases, we set out to test if caspase-2 can function as an initiator caspase in this pathway. Kinetic experiments revealed that caspases-2, -8, -9, but not caspase-1, could be cleaved as early as 5 h after α-toxin treatment in HeLa cells, as analysed by immunoblots (Figure 2A). As predicted, cleavage

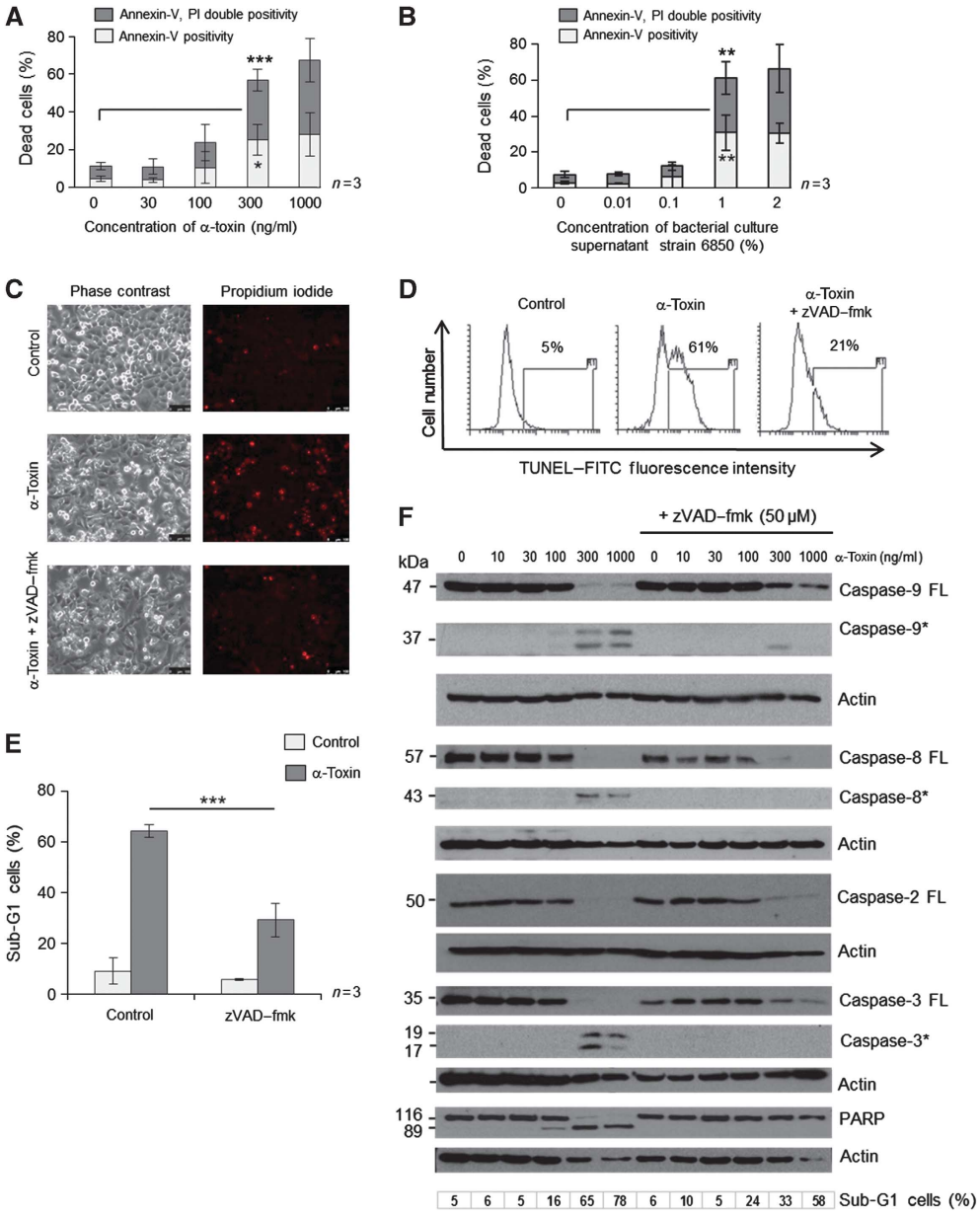

Figure 1 *S. aureus* α-toxin induces caspase-dependent apoptotic cell death in human epithelial cells. HeLa cells were treated with various concentrations of (**A**) purified α-toxin or (**B**) bacterial culture supernatants (from strain 6850) for 24 h. The cells were then subjected to flow cytometric analysis after staining for annexin-V-FITC and propidium iodide, as mentioned in the methods. Dead cells refer to percentage of cells encompassing both annexin-V single-positive (early apoptotic) as well as annexin-V, PI double-positive (late apoptotic) cells. Shown are the data from three independent experiments. (**C**) Microscopic analysis of HeLa cells treated with 300 ng/ml of α-toxin in the presence or absence of zVAD–fmk (50 μM). Shown are representative images of a time-lapse imaging analysis at 24 h after α-toxin treatment. (left panel: phase contrast, right panel: propidium iodide staining in red). (**D**) HeLa cells were treated with α-toxin (300 ng/ml) for 24 h in the presence or absence of zVAD–fmk (50 μM) and the extent of DNA fragmentation was monitored by TUNEL analysis with flow cytometry, as mentioned in the methods section. The percentage of TUNEL-positive cells is gated. (**E**) HeLa cells were treated with α-toxin either alone or with 50 μM of zVAD–fmk, and the cells were subjected to flow cytometric analysis after PI staining to detect the sub-G1 population, as mentioned in the methods section. Shown are data from three independent experiments ± s.d. (**F**) HeLa cells were treated with various concentrations of α-toxin and the processing of various proteins was monitored by western blots. The cells were pretreated with 50 μM of zVAD–fmk to prevent activation of caspases. (FL—full-length protein, *—processed form). The percentage of dead cells (sub-G1 population) in each case is denoted ($* = P < 0.05$, $** = P < 0.01$, $*** = P < 0.005$). Figure source data can be found with the Supplementary data.

of putative caspase-2-specific substrate (VDVAD–fmk) was also observed in α-toxin-treated cells (Figure 2B). As VDVAD–fmk could also be cleaved by other caspases (McStay *et al*, 2008), and as cleavage of the caspase proform is not necessarily an indication of initiator caspase activation, we exploited an *in situ* trapping approach to check for the proximally activated caspase during PFT-mediated apoptosis. This approach has been successfully used before to uncover the initiator caspases during various pathways of apoptosis induction (Tu *et al*, 2006). HeLa cells were loaded with cell-permeable biotin-VAD (biotinylated-Val-Ala-Asp-CH2F) and the cells were subjected to apoptosis induction

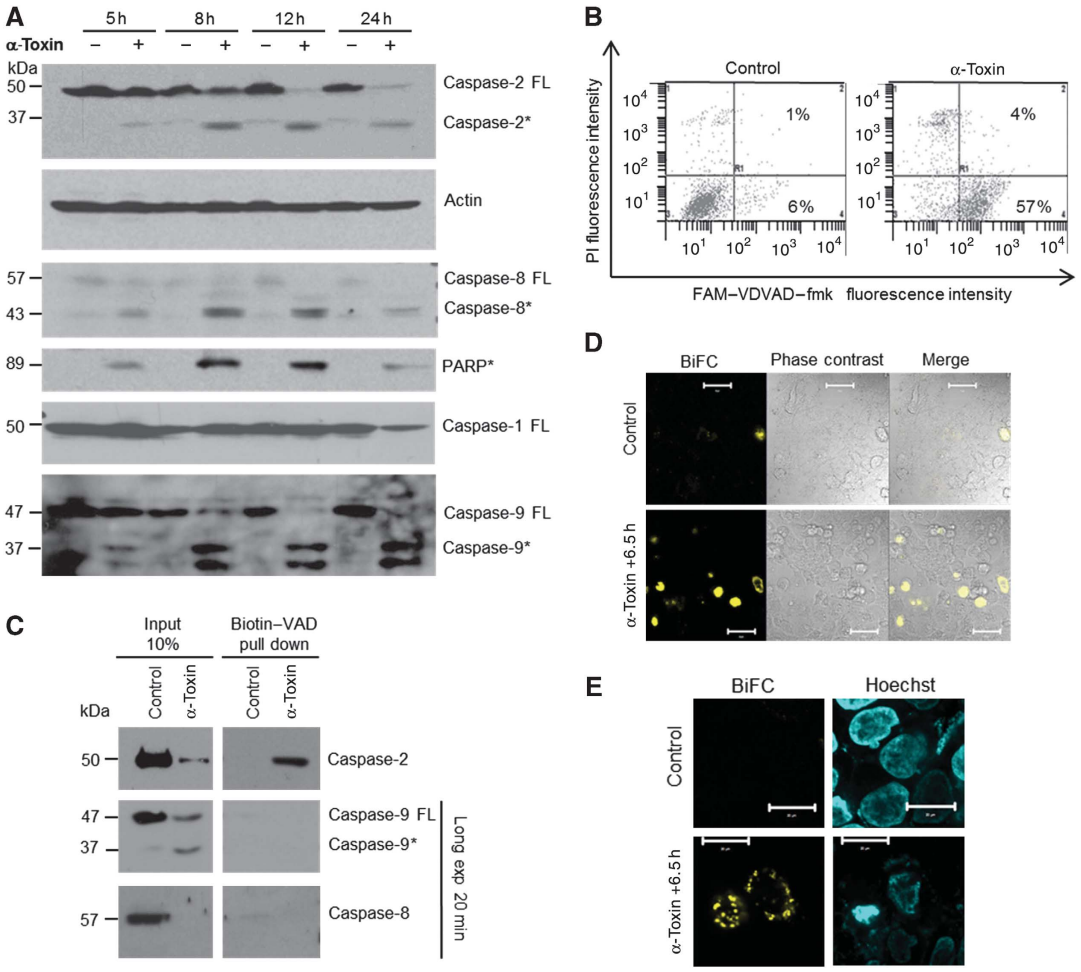

Figure 2 Caspase-2 is the initiator caspase during α-toxin-mediated apoptosis. (**A**) HeLa cells were treated with α-toxin (300 ng/ml) for various time points and the processing of caspases-2, -9, -8, -1 and PARP were monitored by immunoblots. Caspase-2 was detected by monoclonal antibody (clone 11b4; FL—full-length protein, *—processed form). (**B**) Flow cytometric analysis of caspase-2 activity. HeLa cells were incubated with or without α-toxin (300 ng/ml) for 24 h. Percentage of cells displaying caspase-2 activity is denoted. The cells were co-stained with PI to monitor membrane damage. (**C**) HeLa cells pretreated with biotin-VAD and treated with α-toxin as mentioned earlier. The activated caspases are precipitated as mentioned in the methods section. (**D**, **E**) BiFC of caspase-2 CARD. Hela cells transfected with venus–CARD constructs were treated with toxin, and BiFC (yellow) was measured under a confocal microscope. The nuclei are stained with Hoechst (blue) and the overlay is presented. Figure source data can be found with the Supplementary data.

with α-toxin for 6 h. Biotin-VAD that prevented α-toxin-mediated cell death was subsequently precipitated with streptavidin beads and the precipitates were probed with antibodies directed against initiator caspases-8,-9 and -2 (Figure 2C). Interestingly, we could detect only full-length caspase-2 in these precipitates, suggesting that caspase-2 could function as an initiator caspase under these conditions. We have also subjected the whole sample to mass spectrometric analysis. Interestingly, tryptic peptides representing caspase-2, but not from other caspases, were detected in these precipitates (Supplementary Figure S5A). The specificity of the bands recognized by caspase-2 antibody in the B-VAD pull-down samples was further confirmed by using cells expressing validated shRNAs directed against caspase-2 (Supplementary Figure S5B). These experiments revealed that caspase-2 functions as the initiator caspase during PFT-mediated apoptosis in these cell types. As caspase-2 can be activated by effector caspases, we have tested for the activation of caspase-2 in mouse embryonic fibroblasts (MEFs) derived from caspase-3/7 double-deficient mice. Treatment of MEFs with α-toxin failed to induce any cell death possibly due to the lack of α-toxin-binding receptors in these cell types (data not shown). This being the case, we resorted to aerolysin for these experiments. As expected, high caspase-2 activity could be detected in caspase-3/7 double-deficient MEFs (Supplementary Figure S5C), suggesting that activation of caspase-2 is not dependent on effector caspases during PFT-mediated apoptosis. To further confirm the activation of caspase-2 *in situ*, we used bimolecular fluorescence complementation (BiFC) to measure caspase-2 activation upon α-toxin treatment in HeLa cells. As expected, we have obtained strong BiFC signals with caspase-2/CARD constructs that are primarily localized to the cytosol (Figure 2D and E and Supplementary Figure S5D).

Caspase-2 is required during PFT-mediated apoptosis

We then explored, if activation of caspase-2 is required for α-toxin-mediated apoptosis. To address this issue, we established HeLa cell lines stably expressing shRNAs directed against caspase-2. Three out of four specific shRNAs

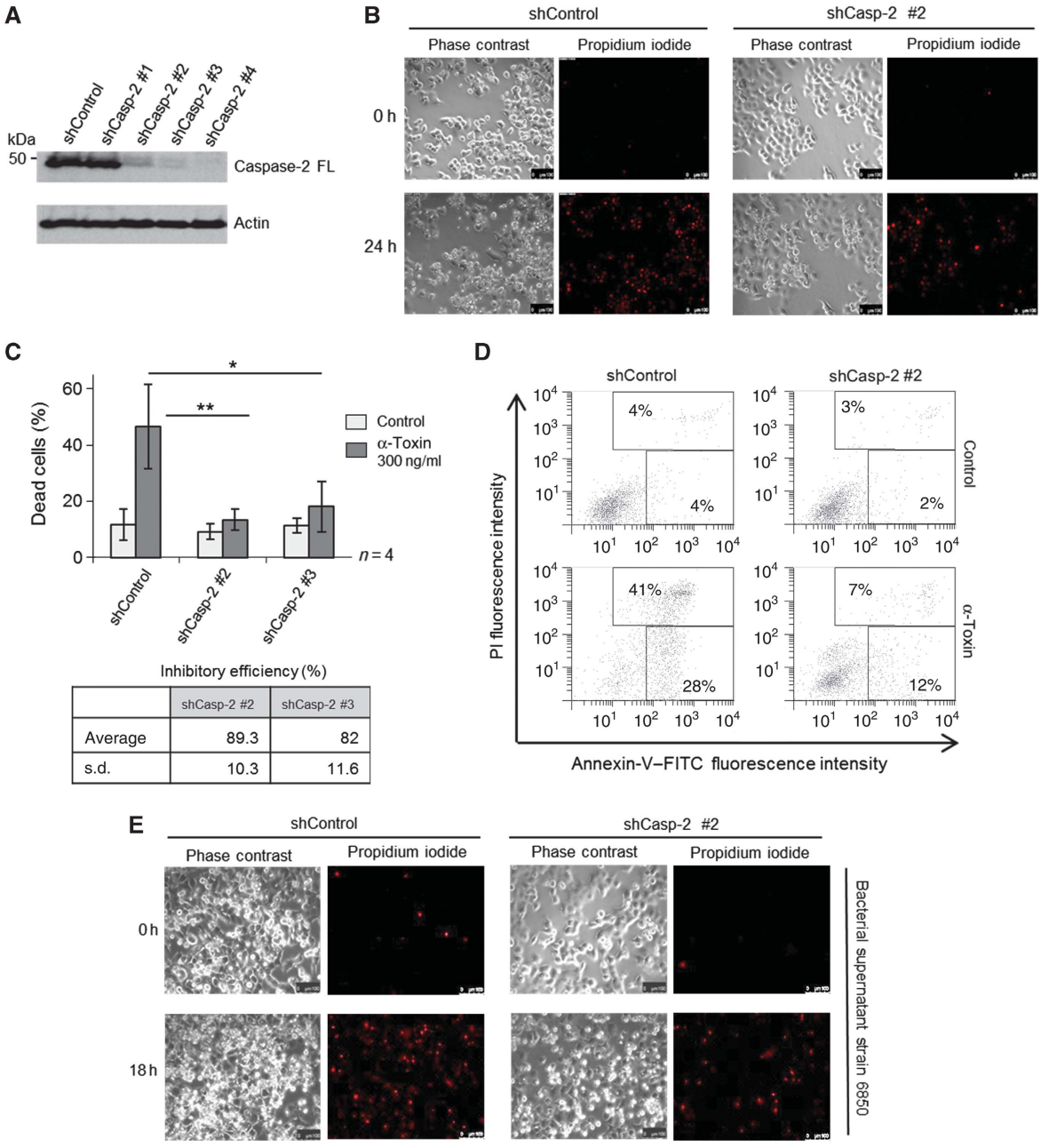

Figure 3 Caspase-2 is required for α-toxin-mediated apoptosis. (**A**) HeLa cells stably expressing various shRNAs directed against caspase-2 or control shRNA were subjected to immunoblot analysis to check for the efficiency of knockdown. Actin was used as a loading control. (**B**) Microscopic analysis of shControl and shCaspase-2 cells to monitor membrane permeabilization after α-toxin (300 ng/ml) treatment. Shown are representative images at 0 and 24 h after toxin treatment from a time-lapse imaging experiment. Shown in left are phase-contrast images, and in right are the identical regions with PI staining (red). (**C**) Flow cytometric analysis of HeLa cells (stably expressing either shControl or two shRNAs directed against caspase-2) treated with α-toxin (300 ng/ml) for 24 h. Percentage of dead cells represents both annexin-V single-positive and annexin-V, PI double-positive cells. The inhibitory efficiency is denoted in the table. Shown are data from four independent experiments. Error bars represent ± s.d. of the mean. (**D**) Representative scatter plots from flow cytometric analysis of control and caspase-2-depleted cells displaying annexin-V, PI staining from **C**. (**E**) Microscopic analysis (left panel: phase contrast, right panel: PI staining—red) of control and caspase-2-depleted HeLa cells treated with bacterial supernatant. shControl and shCaspase-2 #2 cells were incubated with or without bacterial supernatant from stain 6850 (1%, v/v) (* = $P<0.05$, ** = $P<0.01$, *** = $P<0.005$). Figure source data can be found with the Supplementary data.

effectively downregulated the expression of caspase-2 in these cells (Figure 3A). When challenged with α-toxin, caspase-2-deficient cells exhibited profound resistance to cell death, as revealed by two different assays to measure apoptosis (Figure 3B–D). Analysis with time-lapse microscopy also revealed that the structural integrity of the caspase-2-deficient cells was largely preserved despite α-toxin treatment. This effect was profound up to 24–30 h and abated later on (Figure 3B; Supplementary Figure S6A and Supplementary Movies S1 and S2). However, caspase-2-depleted cells still underwent necrosis-like cell death (characterized by loss of membrane integrity and PI incorporation) at later time points, presumably due to persistent damage (Supplementary Figure S6A, Supplementary Movies S1 and S2). Similar results were

obtained when the HeLa cells were challenged with bacterial culture supernatants (Figure 3E and Supplementary Figure S6B). To check if caspase-2 is required for apoptosis induction by other PFTs, we challenged control and caspase-2 knockdown HeLa cells with aerolysin. Depletion of caspase-2 also protected HeLa cells from aerolysin-mediated apoptosis (Figure 4A–C) highlighting its general relevance. To further confirm these observations, we also used MEFs derived from caspase-2-deficient mice. Consistently, loss of caspase-2 prevented MEFs from aerolysin-mediated apoptosis, confirming the crucial role for this caspase in mediating PFT-mediated apoptosis (Figure 4D).

As caspases-8 and -9 are also processed in α-toxin-treated HeLa cells, we tested if these caspases are equally required for eliciting PFT-induced apoptosis. We have validated the efficiency of the shRNA-mediated knockdowns of these caspases in HeLa cells by using positive controls (Supplementary Figure S7A and B). First, shRNA-mediated depletion of either caspase-8 or -9 failed to prevent the processing of caspase-2 in HeLa cells (Figure 5A and B). In contrast, loss of caspase-2 strongly reduced the processing of caspases-8 and -9 (Figure 5C and D). Consistently, depletion of caspase-8 or-9 or both failed to provide any significant protection from α-toxin-mediated apoptosis in these cell types (Figure 5E–H and Supplementary Figure S7 and S8). These data indicate that processing and/or activation of caspases-8 and -9 during PFT-mediated apoptosis are possibly secondary events. This being the case, we have checked for the involvement of proapoptotic Bcl-2 family members, BAK and BAX, during PFT-mediated cell death. Depletion of BAX partially prevented α-toxin-mediated apoptosis in HeLa cells (Supplementary Figure S9A and B). To substantiate these claims, we have used MEFs derived from BAX/BAK double-deficient mice. Loss of both BAX and BAK prevented aerolysin-mediated cell death in these cells (Supplementary Figure S9C). Consistently, depletion of caspase-2 prevented Smac release from the mitochondria in response to α-toxin in HeLa cells (Supplementary Figure S9D). As HeLa cells express caspase-1, we have also tested for the possible role for caspase-1 during PFT-mediated apoptosis in these cells. However, depletion of caspase-1 using shRNAs failed to provide any significant protection from α-toxin-mediated apoptosis (Supplementary Figure S10). Finally, we have tested for the involvement of effector caspases during PFT-mediated apoptosis. Loss of both caspases-3 and -7 largely prevented aerolysin-mediated cell death, revealing a role for effector caspases in regulating PFT-mediated apoptosis (Figure 5I). Taken together, these results confirmed the obligatory role of caspase-2 as an initiator caspase, which in turn activates MOMP and effector caspases to ellicit PFT-mediated apoptotic cell death in epithelial cells and fibroblasts.

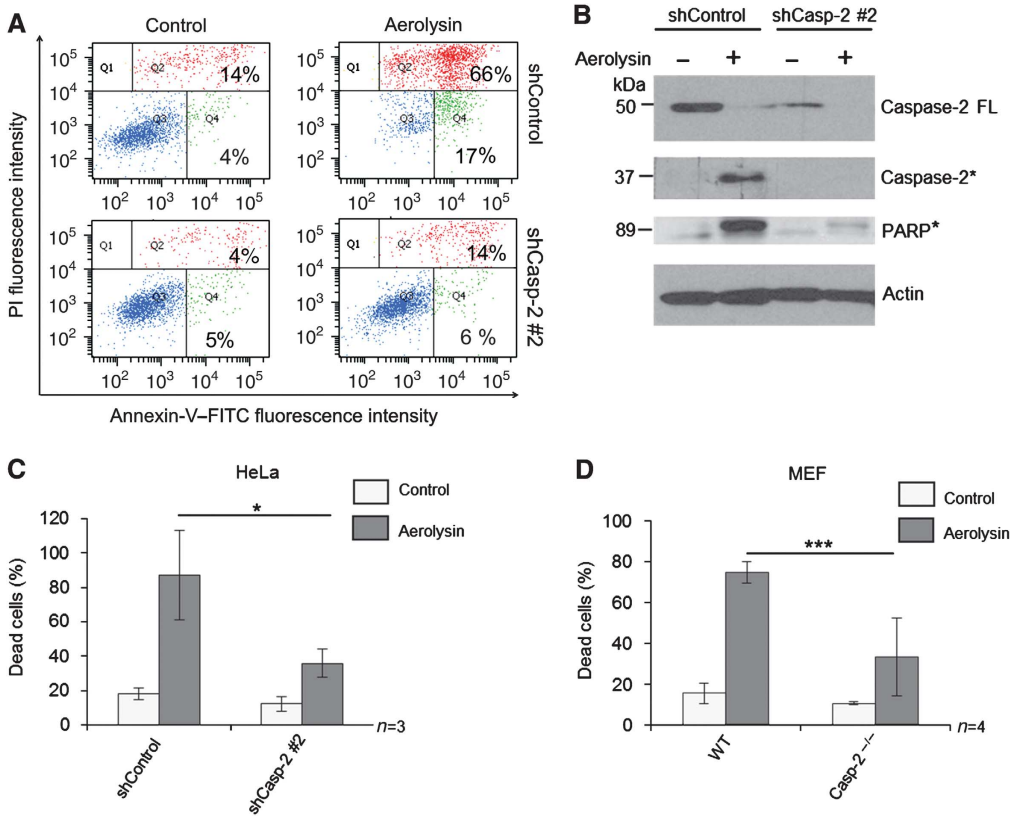

Figure 4 Caspase-2 is required for aerolysin-mediated apoptosis. (**A**) Representative dot plots of flow cytometric analysis of control and caspase-2-knockdown cells upon aerolysin toxin treatment (5 ng/ml for 48 h). Cells were subjected to annexin-V and PI staining and the percentage of cells displaying annexin-V single positivity (Q4) and annexin-V, PI double positivity (Q2) are denoted. (**B**) Western blot analysis of HeLa cells treated with aerolysin for 24 h. The processing of caspase-2 and PARP was monitored (FL—full-length protein, *—processed form). (**C**) Flow cytometric analysis of caspase-2-knockdown HeLa cells 48 h after aerolysin (5 ng/ml) treatment and (**D**) Caspase-2-/- MEFs 24 h after aerolysin (5 ng/ml) treatment. Percentage of dead cells represents the percentage of cells displaying both annexin-V single positivity and annexin-V, PI double positivity out of the total number of cells (* = $P<0.05$, ** = $P<0.01$, *** = $P<0.005$). Figure source data can be found with the Supplementary data.

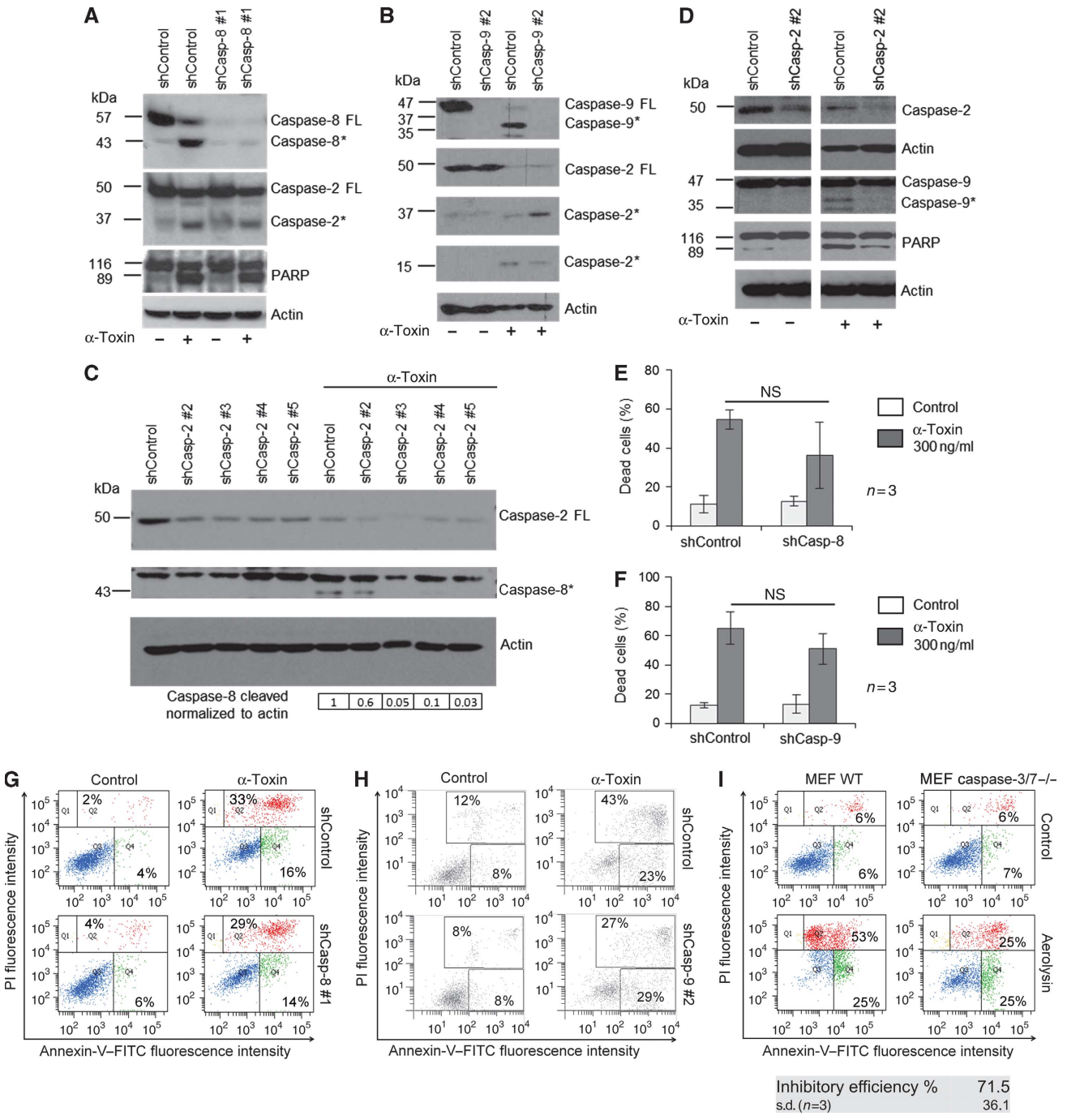

Figure 5 Caspases-8 and -9 are not required for α-toxin-mediated apoptosis. (**A**) Western blot detection of caspase-2 processing in shControl and shCaspase-8 cells, and in (**B**) shControl and shCaspase-9 cells after α-toxin treatment (300 ng/ml, 24 h). (**C**) Western blot analysis of caspase-8 and (**D**) caspase-9 cleavage in shControl and shCaspase-2 cells. The cells were treated with α-toxin (300 ng/ml, 24 h). Cleavage of PARP was monitored and actin was used as a loading control. (**E**, **F**) represents the percentage of cells exhibiting both annexin-V single positivity and annexin-V, PI double positivity compared to the total number of cells. (**G** and **H**) Representative scatter plots of cell death analysis in (**E**) caspase-8 and (**F**) caspase-9-knockdown cells. ShControl and shCasp-8 #1 or shCasp-9 #2 cells were incubated with or without α-toxin (300 ng/ml) for 24 h, respectively, and subjected to annexin-V, PI staining and flow cytometry analysis (NS—not significant). (**I**) Wild-type and caspase-3/7 double-deficient MEFs were challenged with aerolysin, and cell death was measured by annexin-V, PI analysis. Shown are data from one representative experiment. The inhibition efficiency is ~71.5% ($n = 3$). Figure source data can be found with the Supplementary data.

Activation of caspase-2 is PIDDosome independent

We then explored the mechanisms behind activation of caspase-2 during PFT-mediated apoptosis. As mentioned before, multimerization of initiator caspases in HMW complexes is required for the activation of initiator caspases during various pathways of apoptosis induction. Caspase-2 has been previously shown to be activated by the formation of PIDDosome during DNA damage-mediated apoptosis (Tinel and Tschopp, 2004). However, recent studies revealed that caspase-2 activation can happen in the absence of PIDDosome components (Manzl *et al*, 2009). We initially checked if PIDD and RAIDD are required for PFT-

mediated caspase-2 activation. Interestingly, depletion of RAIDD or PIDD failed to prevent α-toxin-mediated apoptosis (Figure 6A–D). As expected, the cleavage of caspase-2 in response to α-toxin was not prevented by the depletion of either PIDD or RAIDD (Figure 6E and F). Consistently, biotin-VAD pull-down experiments revealed that caspase-2 could be activated in the absence of RAIDD in response to α-toxin (Figure 6G). To further confirm these observations, we challenged PIDD-deficient MEFs with pro-aerolysin, and as predicted, loss of PIDD failed to prevent aerolysin-mediated apoptosis in MEFs (Supplementary Figure S11). These results confirmed that activation of caspase-2 in response to PFTs is independent of PIDD or RAIDD.

Caspase-2 is recruited to a HMW complex in toxin-treated cells

Previous studies have shown that full-length caspase-2 can be recruited to a HMW PIDDosome complex in a cell-free system in response to temperature shift (Read *et al*, 2002; Tinel and Tschopp, 2004). However, whether any such caspase-2-containing HMW complexes exist under physiological conditions in apoptotic cells is not known so far. As caspase-2 activation is independent of PIDD and RAIDD, we set out to investigate if endogenous caspase-2 is recruited to any HMW complexes in toxin-treated cells. We performed gel filtration analysis on HeLa cell extracts derived from control and α-toxin-treated cells in search of any such caspase-2-containing complexes. Immunoblotting of proteins obtained in the individual fractions after separation on a Superose 6 10/300 GL column revealed that caspase-2 is recruited to HMW complex of >1 MDa in α-toxin-treated cells (Supplementary Figure S12). Interestingly, we detected the intermediate form of cleaved caspase-2 in the HMW complexes in α-toxin-treated cells, suggesting the presence of active caspase-2 in these fractions (Supplementary Figure S12). Compared to the full-length caspase, this activated form was also much less populated in fractions corresponding to molecular weights between 100 and 200 kDa and eluted mainly as a monomer.

The Superose 6 10/300 GL column, however, does not allow us to distinguish between a real HMW complex and aggregated proteins, as the elution maximum is close to the void volume of the column. To answer this question and to obtain a better estimation of the size of the caspase-2-containing HMW complexes, we used a Sephacryl S-500 HR column. These analysis revealed that caspase-2 is reproducibly recruited to HMW complex eluting significantly earlier than single ribosomes, with a maximum in fraction #12 corresponding to an elution volume of 63–66 ml and a calculated Stokes radius of about 32.5–36.5 nm. We have consistently detected either the intermediate and/or the fully processed forms of caspase-2 in fraction 12 in α-toxin-treated HeLa cells (Figure 6H and Supplementary Figure S13). Interestingly, we could detect the full-length form of caspase-2 in fraction 12 in α-toxin-treated cells, suggesting that caspase-2 might be recruited to this complex for its activation and processing (Figure 6H). As predicted, RAIDD or PIDD is not detectable in these HMW complexes, suggesting that RAIDD and PIDD are possibly not involved in the recruitment and oligomerization of caspase-2 to HMW complexes at endogenous levels under these conditions (Supplementary Figure S13).

Potassium efflux elicited by PFTs regulates caspase-2 activation

We then explored the molecular mechanisms behind α-toxin-mediated activation of caspase-2. PFTs have been shown to cause membrane injury and selective depletion of potassium ions (Bischofberger *et al*, 2009; Gonzalez *et al*, 2011), which in turn contributes to inflammasome-dependent caspase-1 activation in macrophages (Walev *et al*, 1995; Gurcel *et al*, 2006). We analysed for potassium ion concentrations in α-toxin-treated HeLa cells and, as predicted, we could detect a significant decrease in endogenous K^+ ion concentrations in α-toxin-treated cells (Figure 7A). To check if K^+ efflux contributes to caspase-2 activation, the cells were cultured in high potassium-containing media before being subjected to α-toxin treatment, and the selectivity and efficiency of K^+ efflux inhibition has been tested (Supplementary Figure S14A). Interestingly, inhibition of potassium efflux prevented α-toxin-mediated caspase-2 activation (Figure 7B and C). Consistently, cell death induced by α-toxin was also prevented when the cells were cultured in media containing high potassium ion concentrations, as measured by two different assays (Figure 7D–F). We then investigated if potassium ion levels contribute to the recruitment of caspase-2 to HMW complexes at endogenous levels. Consistently, culturing cells in high potassium-containing media prevented the recruitment of caspase-2 to HMW complexes in α-toxin-treated HeLa cells (Figure 7G). These results revealed a crucial role for potassium ion concentrations in the

Figure 6 α-Toxin-mediated caspase-2 activation is independent of PIDDosome. HeLa cells stably expressing scrambled control or RAIDD shRNAs are treated with or without α-toxin (300 ng/ml) for 8 h and subjected to Sub-G1 or treated for 24 h and subjected to annexin-V, PI staining. Percentage of cells representing sub-G1 population is presented in **A**, and the percentage of cells displaying both annexin-V single positivity and annexin-V, PI double positivity is presented in **B**. Shown are data from three independent experiments. Error bars represent ± s.d. of the mean. (**C**) Representative experiment from sub-G1 analysis of control and PIDD-depleted cells after α-toxin treatment (8 h, 300 ng/ml). (**D**) Control and PIDD-depleted HeLa cells were treated with α-toxin (24 h, 300 ng/ml) and the percentage of cells displaying annexin-V single positivity and annexin-V, PI double positivity is depicted. Shown are data from three independent experiments (NS—not significant). HeLa cells stably expressing control or RAIDD (**E**) or PIDD (**F**) shRNAs were subjected to α-toxin treatment (24 h, 300 ng/ml), and processing of caspase-2 was monitored by immunoblots. (FL—full-length protein, *—processed form). (**G**) Control and RAIDD-depleted HeLa cells were subjected to biotin-VAD analysis, as mentioned in the methods section. The presence of caspase-2 was monitored in the biotin-VAD (B-VAD) precipitates by immunoblot analysis (# denoted the higher exposure of blots presented above). (**H**) Western blot analysis of various fractions obtained after size exclusion chromatography. Cell lysates from HeLa cells treated with or without α-toxin (8 h, 300 ng/ml) are subjected to gel filtration analysis, as mentioned in the methods section. The proteins in the individual fractions were precipitated with TCA, and the presence of caspase-2 was monitored by immunoblot analysis, as mentioned in the methods section. Processed form of caspase-2 consistently eluted in fraction #12 in α-toxin-treated cells. Single ribosomes ($\sim$2.3 MDa) eluted around fractions 16–17. The occurrence of processed protease in non-treated cell lysates is most likely caused by the sample handling during preparation for the gel filtration experiment, as basically no activated caspase-2 is visible in the lane of a sample frozen directly after cell lysis (input lane) or in western blot shown in Figure 2A. Figure source data can be found with the Supplementary data.

recruitment of caspase-2 to HMW complexes at endogenous levels. Taken together, these results revealed that potassium efflux by PFTs contributes to caspase-2 activation in epithelial cells to induce apoptosis (Figure 7H). To further confirm these observations we have treated the cells with potassium ionophone Nigericin. Nigericin treatment led to caspase-2 activity in more than 80% of cells, and consistently loss of caspase-2 prevented Nigericin-mediated cell death (Supplementary Figure S14B and C). These data confirm the crucial role of potassium ion concentrations in regulating the activation of caspase-2 and cell death in these cell types.

Discussion

Numerous bacterial pathogens have been shown to modulate host cell apoptosis to establish successful infection (Lamkanfi

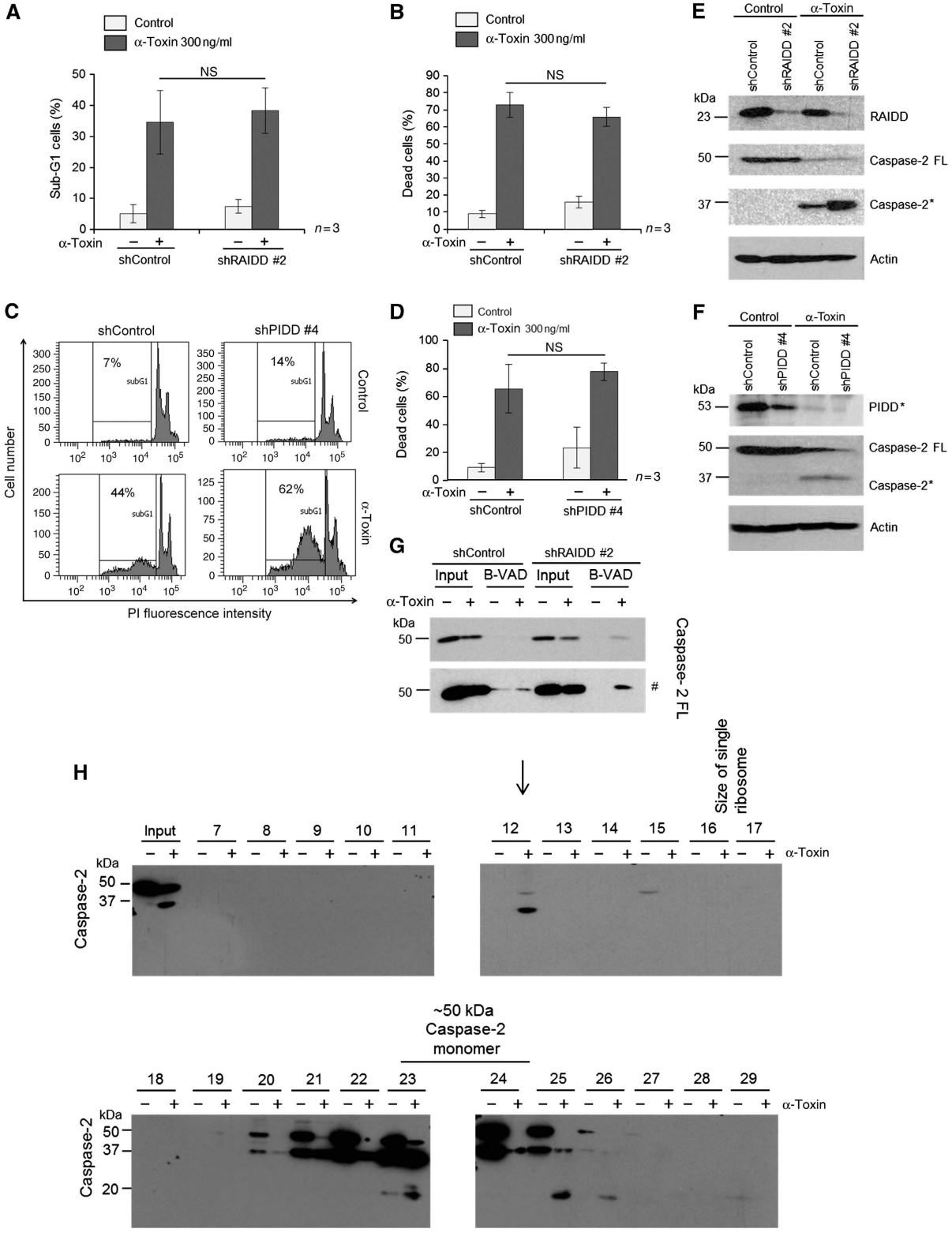

and Dixit, 2010). In the case of *S. aureus*, induction of cell death could contribute to both tissue damage as well as to escape immune response. Previous studies have shown that the soluble secreted factor α-toxin is the major factor responsible for triggering apoptotic cell death in various immune cells (Bantel *et al*, 2001). PFTs are a major class of bacterial virulent factors and formation of pores is a widely employed means of cellular attack, and pathogens have evolved numerous toxins to circumvent host defence to establish successful infection (Bischofberger *et al*, 2009). However, host cells have also evolved counter-attack mechanisms to promote membrane repair, toxin removal,

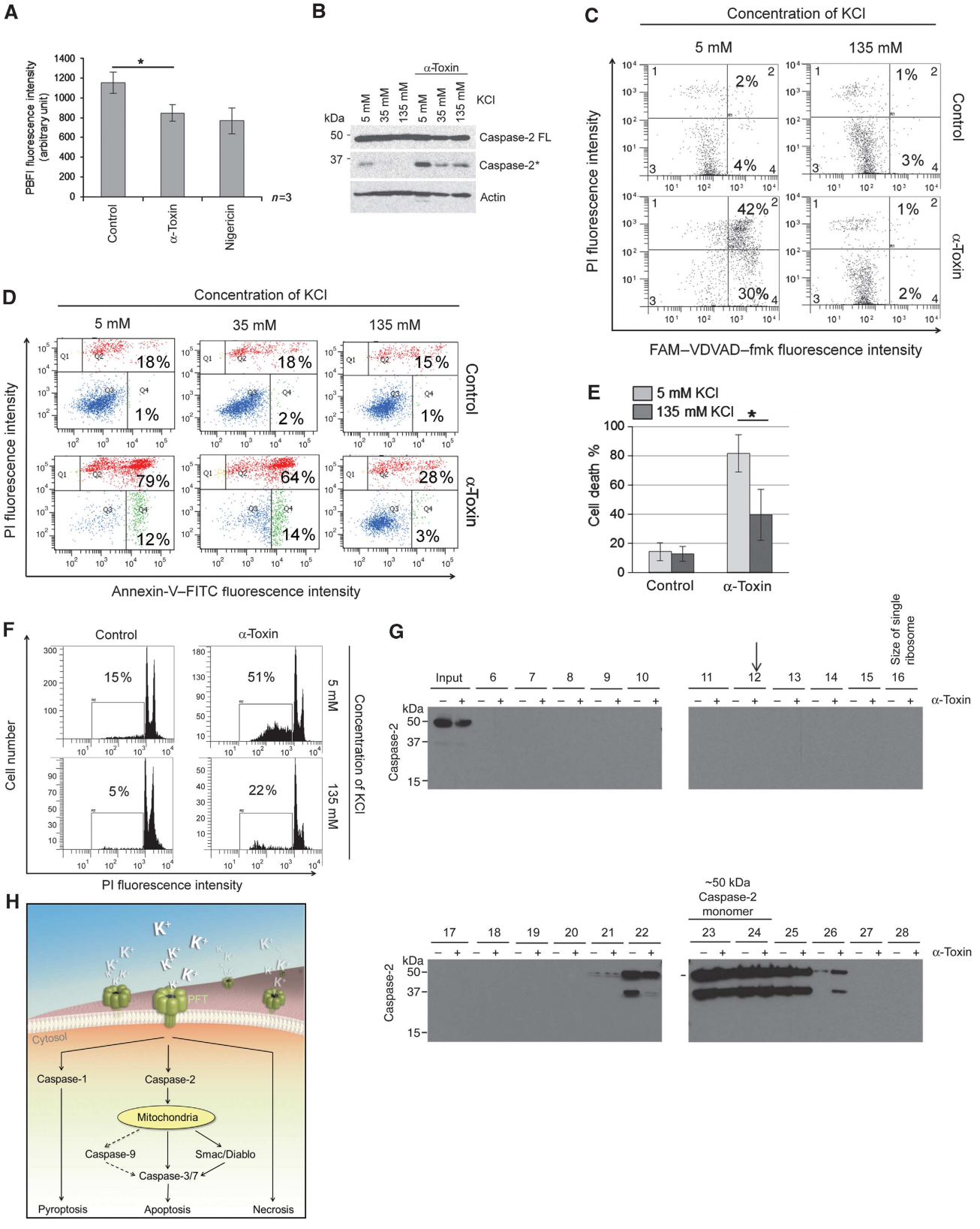

autophagy and promoting cell survival through activation of multiple kinase pathways (Bischofberger *et al*, 2009; Husmann *et al*, 2009; Draeger *et al*, 2011). If the damage is persistent and irreparable, the cells undergo either programmed or non-programmed cell death. While erythrocytes and macrophages undergo osmotic lysis or pyroptosis with *S. aureus* α-toxin, respectively (Bhakdi and Tranum-Jensen, 1991; Gonzalez *et al*, 2008), the molecular mechanisms for PFT-mediated cell death in epithelial cells and keratinocytes, one prime site of pathogen entry, are just emerging. Our studies unveil the molecular machinery driving PFT-mediated apoptotic cell death in epithelial cells, including primary cells, and surprisingly revealed an obligatory role for caspase-2 (Figure 7H).

Caspase-2 contains a CARD domain, which is typical of initiator caspases (Baliga *et al*, 2004) and also exhibit some properties of effector caspases (Krumschnabel *et al*, 2009). During development, caspase-2 has been shown to be required for oocyte apoptosis in xenopus (Nutt *et al*, 2005, 2009). Previous studies have unveiled a role of caspase-2 as an initiator caspase during heat-shock- and DNA damage-mediated apoptosis (Tu *et al*, 2006; Krumschnabel *et al*, 2009). Caspase-2 interacts with RAIDD through the CARD domain and indirectly with PIDD to constitute the PIDDosome, which could serve as a platform for its activation during genotoxic stress (Tinel and Tschopp, 2004). However, recent studies revealed that PIDD and RAIDD are dispensable for apoptosis induction by a wide range of stimuli in mammalian cells (Manzl *et al*, 2009). These studies also revealed that caspase-2 can be activated in a PIDD/RAIDD-independent manner. Further, caspase-2 can also be recruited to DISC upon FAS ligation in T- and B-cell lines (Lavrik *et al*, 2006). Despite these observations, the unique apoptotic stimuli that require caspase-2 as an initiator caspase remain elusive so far.

Our data suggest that caspase-2 functions as an initiator caspase during PFT-mediated apoptosis in epithelial cells. Interestingly, caspases-8 and -9 though processed during toxin-mediated apoptosis are not necessary for mediating cell death, at least in these cell types. Previous studies have, however, revealed a role for these caspases during PFT-mediated cell death in other cell types (Bantel *et al*, 2001; Haslinger *et al*, 2003). We have also utilized '*in situ*-trapping' approach using biotin-VAD to reveal that caspase-2 is the first activated caspase in response to α-toxin. Caspase-2 activation occurs upstream of mitochondria, as caspase-8 or-9 or effector caspases are not required for its activation and the release of mitochondrial proteins like Smac/DIABLO is reduced in caspase-2-depleted cells in response to α-toxin (Figure 5 and Supplementary Figure S9D). Consistently, loss of function analysis employing multiple shRNAs or genetic deletion unveils the obligatory role for this caspase during PFT-mediated apoptosis. However, there is a clear requirement of MOMP in this process, which could contribute to effector caspase activation by the release of natural IAP antagonists. Interestingly, despite strong expression, caspase-1 is not required for mediating apoptosis by PFTs in these cells, which suggests that unique caspases are activated in a cell type-dependent manner to elicit various modes of cell death.

Our experiments with BiFC reveal that dimerization of caspase-2 happens predominantly in the cytosol, consistent to the previous observations made during heat-shock-mediated apoptosis (Bouchier-Hayes *et al*, 2009). We further unveil the crucial role of potassium ions in regulating the recruitment and activation of caspase-2 in human cells. Previous studies have also revealed that physiological levels of KCl or NaCl prevent the formation of apoptosome and caspase-2 activation *in vitro* (Thompson *et al*, 2001; Read *et al*, 2002). Depletion of potassium ions in response to PFTs could therefore trigger the oligomerization of caspase-2 in the presence or absence of any putative adaptor proteins for its activation. However, the presence of caspase-2 in a HMW complex in apoptotic cells clearly indicates the possible presence of other proteins in this complex. The exact composition of the complex, the stoichiometry and the functionality of the constituent proteins in the activation of caspase-2 need to be further elucidated. As PFT-mediated cell death requires BAX and BAK, the specific BH3-only proteins required to activate MOMP under these settings remain unclear. Though we could not detect any significant processing of Bid, one cannot rule out a role for this BH3 family member as it has been shown to be activated by caspases. The specific role for BH3-only family members in accomplishing MOMP downstream of caspase-2 activation needs to be addressed. In the same lines, how K^+ efflux elicited by PFTs contributes to the assemblage of caspase-2 activation complexes deserves further studies. As caspase-2 activation is also detected during *Brucella* and *Salmonella* infections (Jesenberger *et al*, 2000; Chen and He, 2009), targeting caspase-2 could be exploited as a therapeutic strategy to control pathogenesis of specific infection-related disorders.

Materials and methods

shRNA-mediated RNA interference

In order to silence the expression of caspases-1, -2, -8, -9, BAX, PIDD and RAIDD by shRNAs, approximately 40 000 cells/well were

Figure 7 Potassium efflux is required for α-toxin-mediated caspase-2 activation and apoptosis. (**A**) HeLa cells were treated with solvent, α-toxin (300 ng/ml) or nigericin for 5 h, and intracellular potassium levels were analysed by measuring PBFI fluorescence as mentioned in the methods section. Shown are data from three independent experiments. (**B**) HeLa cells were cultured in media with various potassium ion (KCl) concentrations before α-toxin treatment (24 h, 300 ng/ml) and subjected to various analyses. The cleavage of caspase-2 is monitored by immunoblot. (**C**) Activation of caspase-2 was measured by FAM-VDVAD fluorescence. (**D**, **E**) Annexin-V, PI detection or (**F**) appearance of sub-G1 population as measured by flow cytometric analysis, respectively. Panels **D** and **F** are representative experiments. (**G**) HeLa cells were cultured in high potassium media (135 mM KCl) and then treated with α-toxin (8 h, 300 ng/ml). Cell lysates were prepared and then subjected to gel filtration analysis as in Figure 6H. The presence of caspase-2 in various fractions was monitored by immunoblots. The arrow indicates the position where the HMW complex would be expected. The occurrence of processed protease in the fractions 22–26, despite the absence of activated caspase-2 in the input sample again, suggests that processing occurs during the preparation for the gel filtration experiment. However, the absence of a signal in lane 12 shows that only caspase-2 modified in intact cells is capable of forming this HMW complex. (**H**) Scheme of PFT induced cell death pathways. Pore-forming toxin elicits various forms of cell death, depending on concentrations and cell types. PFT-mediated apoptosis in epithelial cells is dependent on caspase-2. Loss of caspase prevents PFT-mediated cell death, and potassium ion depletion contributes to caspase-2 activation, which is independent of PIDD and RAIDD ($* = P < 0.05$, $** = P < 0.01$, $*** = P < 0.005$). Figure source data can be found with the Supplementary data.

seeded in a 96-well plate 24 h before infection. Lentiviral particles carrying shRNAs directed against various genes and scrambled control shRNAs were added to the cells as per manufacturer's instructions (Sigma). At 24 h after infection, media was changed, and at 48 h after infection, cells were trypsinized and transferred to 12-well plates and subjected to selection of puromycin-resistant cells (final concentration: 2.5 μg/ml). In all the experiments described, knockdown efficiency was verified and pool of cells was used to avoid clonogenic effects. The knockdown efficiency was validated by western blot analysis.

The following sequences have been used to silence the expression of various genes:

Caspase-2 #2 (TRCN0000003506):
5′-CCGGCACTCCCTAGACAATAAAGATCTCGAGATCTTTATTGTCTAGGGAGTGTTTTT-3′

Caspase-2 #3 (TRCN0000003507):
5′-CCGGCTAGTCACCCTCTTCAAGCTTCTCGAGAAGCTTGAAGAGGGTGACTAGTTTTT-3′

Caspase-2 #4 (TRCN0000003508):
5′-CCGGGTTGAGCTGTGACTACGACTTCTCGAGAAGTCGTAGTCACAGCTCAACTTTTT-3′

Caspase-2 #5 (TRCN0000003509):
5′-CCGGGATATGTTGCTCACCACCCTTCTCGAGAAGGGTGGTGAGCAACATATCTTTTT-3′

Caspase-8 #1 (TRCN0000003575):
5′-CCGGGAATCACAGACTTTGGACAAACTCGAGTTTGTCCAAAGTCTGTGATTCTTTTT-3′

Caspase-9 #2 (TRCN0000003581):
5′-CCGGCAGCTTCCAGATTGACGACAACTCGAGTTGTCGTCAATCTGGAAGCTGTTTTT-3′

RAIDD #2 (TRCN0000107207):
5′-CCGGGACGGATATCTACCGCTGTAACTCGAGTTACAGCGGTAGATATCCGTCTTTTTG-3′

PIDD #4 (TRCN0000165220):
5′-CCGGGCACCTGAAGAATGTGAAGGACTCGAGTCCTTCACATTCTTCAGGTGCTTTTTTG-3′

BAX #2 (TRCN00000033469):
5′-CCGGGATGTGGTCTATAATGCGTTTCTCGAGAAACGCATTATAGACCACATCTTTTTG-3′

BAX #3 (TRCN00000033470):
5′-CCGGGCCCACCAGCTCTGAGCAGATCTCGAGATCTGCTCAGAGCTGGTGGGCTTTTTG-3′

Caspase-1 #1 (TRCN0000003502):
5′-CCGGCCAGATATACTACAACTCAATCTCGAGATTGAGTTGTAGTATATCTGGTTTTT-3′

Caspase-1 #2 (TRCN0000003503):
5′-CCGGCTACAACTCAATGCAATCTTTCTCGAGAAAGATTGCATTGAGTTGTAGTTTTT-3′

Caspase-1 #3 (TRCN0000003504):
5′-CCGGCACACGTCTTGCTCTCATTATCTCGAGATAATGAGAGCAA\GACGTGTGTTTTT-3′

Caspase-1 #5 (TRCN0000010796):
5′-CCGGGAAGAGTTTGAGGATGATGCTCTCGAGAGCATCATCCTCAAACTCTTCTTTTT-3′

ShControl: (SHC002V), non-target shRNA control transduction particles.

SiRNA transfection

HeLa cells were plated into 12-well plates to obtain 50–60% confluency at the next day. Hyperfect (Qiagen) reagent was used to achieve siRNA (siRNA Caspase-8 #1 SI02661946, siRNA Caspase-8 #2 SI02662457, Qiagen) transfection as per manufacturers instructions (final DNA concentration: 60 nM). Next day, media was changed and cells were treated with α-toxin. After 24 h, samples were subjected to western blot analysis and flow cytometry detection.

Flow cytometry assays to measure cell death

For the flow cytometry analysis the following channels were used: FITC-FL1 channel (488-nm blue laser/530-nm band-pass filter), PI-FL2 channel (488-nm blue laser/585-nm band-pass filter; BD FACScalibur and FACSCanto II, Becton Dickinson).

Visualizing caspase-2 CARD dimerization with BiFC

These experiments are conducted as described in the study by Bouchier-Hayes *et al* (2009). In short, HeLa cells (seeded in Ibidi eight-well chamber slides) were transfected at the same time with two different plasmids containing the DNA sequence of Caspase-2 CARD domain (1–122 aa), furthermore one of these constructs possessed only the N-terminus, while the other only the C-terminal part of VENUS fluorescent protein sequence (100 ng pBiFC–HA–Caspase-2 CARD-VC155, 100 ng pBiFC–FLAG–Caspase-2 CARD-VN173). The plasmid constructs were transfected with lipofectamine-2000 method, as per manufacturer instructions (Invitrogen). The media was changed 36 h later. Afterwards the cells were induced to undergo apoptosis with α-toxin, and the BiFC fluorescence increase due to the tight proximity of the complementary fluorescent compounds resulted from CARD dimerization was monitored under a confocal microscopy (excitation: 523 nm). For obtaining nuclear staining Hoechst 33342 dye (Sigma; final concentration 1 μg/ml) was applied (excitation: 358 nm).

Measuring sub-G1 population

The appearance of sub-G1 population of cells was monitored to measure apoptosis. Samples were prepared according to a procedure previously published (Gong *et al*, 1994). Briefly, control and α-toxin-treated cells were centrifuged (300 *g*/2 min) and the pellets were resuspended in 1 ml of 70% ethanol ($-20\,^{\circ}C$). The cells were fixed at room temperature for 30 min and stored at $-20\,^{\circ}C$ overnight. Oligonucleosomal DNA fragments were extracted from ethanol-fixed cells in 1 ml of extraction buffer containing 200 mM Na_2HPO_4/citric acid (pH 7.8) and 10 μg/ml RNAse A (Sigma) for 15 min, then stained with PI (propidium iodide (Sigma), 5 μg/ml for final concentration) for 15 min before measurement. Cells were gated to exclude the debris and analysed by flow cytometry.

Annexin-V/PI staining

Control and toxin-treated cells (0.5×10^6 cells) were collected by trypsinization. Samples were washed once with PBS and then resuspended in 100 μl of 1 × annexin binding buffer provided by the manufacturer (Alexis), and then 5 μl of annexin-V-FITC stock solution (Alexis) and 1 μg/ml (final) propidium iodide (PI) were added to the cells and incubated for 15 min. After incubation, the stained samples were measured by flow cytometry. The debris was excluded from analysis.

Caspase-2 activity assay

The activation of caspases was measured by FLICA caspase activity assay kit, strictly following manufacturer's instructions (Immunochemistry Technologies, LLC). Caspase-2 substrate FAM-VDVAD–fmk was used.

TUNEL assay

Control and α-toxin-treated cells were collected by centrifugation, and the cells were subjected to TUNEL staining by following manufacturer's instructions (Promega). The presence of TUNEL-positive cells were monitored and quantified by flow cytometry analysis.

Biotin-VAD pull down of activated caspases

HeLa cells either with or without shRNAs were seeded into 10-cm dishes and were allowed to grow until 80–90% confluency. They were treated with 50 μM biotin-VAD (MP Biomedicals, Enzyme System Products) for 1 h and then 300 ng/ml of α-toxin was added to the cells. The cells were incubated for 6 h and then collected by scraping. The collected cells were washed with PBS and resuspended in 500 μl KPM buffer (50 mM KCl, 50 mM HEPES, 10 mM EGTA, 1.92 mM $MgCl_2$, pH 7.0, 1 mM DTT and 1 × protease inhibitor cocktail (Roche)). The cells were lysed by freezing-thawing (3 ×) and centrifuged for 10 min (15 000 *g*, 4 °C). A quantity of 50 μl of the supernatant was collected as loading control. The rest of the sample (450 μl) was incubated with 30 μl of streptavidin agarose beads (Invitrogen) at 4 °C on a vertical rotator over night. On the next day, samples were centrifuged (2300 r.p.m., 3 min, 4 °C) and the supernatant was thoroughly discarded and the beads were resuspended in 500 μl of KPM buffer. This step was repeated three times. Finally, beads were resuspended in 60 μl of 5 × Laemmli buffer with β-mercaptoethanol. The samples were boiled and subjected to SDS–PAGE for subsequent immunoblot or mass spectrometric analysis.

Immunoblot analysis

Cells were lysed directly in 5 × Laemmli (with 5% β-mercaptoethanol) buffer and the proteins were separated by SDS–PAGE. The proteins were transferred to nitrocellulose membranes (90 min, 860 mA) and the presence of various proteins was monitored by immunoblot analysis following standard procedures. The following antibodies are used: rat anti-caspase-2 11b4clone (Alexis), rabbit anti-caspase-3, mouse anti-caspase-8, rabbit anti-caspase-9, monoclonal rabbit anti-caspase-1 D7F10 clone, rabbit anti-BID, mouse anti-Smac/Diablo and anti-PARP antibodies (Cell Signaling Technologies), rabbit monoclonal anti-RAIDD (Epitomics), mouse monoclonal anti-PIDD (Alexis), rabbit anti-BAX (Millipore), mouse anti-M2-PK (Schebo Biotech) and rabbit anti-actin (Sigma).

Size exclusion chromatography

HeLa cells were grown to 80–90% confluency (six 75-cm^2 flasks per condition) and the cells were treated with α-toxin (300 ng/ml). Depending on the experiment, 5 or 8 h later the cells were collected by scraping, the media was collected in the same tube and samples were centrifuged, washed with PBS and dissolved in 1.2 ml hypotonic buffer (20 mM HEPES, 10 mM KCl, 1 mM $MgCl_2$, 1 mM EDTA, 1 mM EGTA pH 7.5; protease inhibitor cocktail (Roche) 1 × and 1 mM DTT was freshly added) by pipetting up and down as described previously (Read *et al*, 2002). Then the samples were lysed by three times repeated freezing-thawing and centrifuged again. The supernatant was collected to a fresh tube. A quantity of 100 μl of sample was mixed with 5 × Laemmli buffer (with 5% β-mercaptoethanol) and used as total lysate control. The rest (1.1 ml) was subjected to gel filtration. Samples of 1 ml from supernatant of lysed cells were applied onto a HiPrep 16/60 Sephacryl S-500 HR gel filtration column with 120 ml bed volume (GE Healthcare) and separated at a flow rate of 0.5 ml/min. Starting 0.25 CV after injection, 3 ml fractions were taken and analysed by western blotting following TCA precipitation. Only fractions separated from the void volume by more than 0.1 column volumes were considered. The following standards were used for calibration of the column, considering the elution volume (V_e) as a function of the Stokes radius (elution volumes from two measurements): ovalbumin (3.05 nm; 93.13 ml), thyroglobulin (8.5 nm; 81.89 ml) and single ribosomes (20 nm; 77.76 ml). For each standard $K_{av} = (V_e - V_o)/(V_t - V_o)$ was calculated, and the Stokes radius of caspase-2-containing HMW complex was determined by plotting the Stokes radii of the standards versus $(-\log K_{av})^{1/2}$.

In initial size exclusion experiments, 200 μl of supernatant from cell lysis was separated over a Superose 6 10/300 GL column with 23.5 ml total volume (V_t; GE Healthcare) at a flow rate of 0.5 ml/min with fractionation in steps of 500 μl starting immediately after injection. This column was calibrated according to the elution volumes (V_e) of the following standard proteins: ribonuclease A (13.7 kDa; 19.24 ml), ovalbumin (43 kDa; 15.76 ml), albumin (67 kDa; 15.31 ml), catalase (232 kDa; 14.34 ml), ferritin (440 kDa; 12.75 ml) and thyroglobulin (669 kDa; 11.25 ml). The void volume (V_o) was 6.8 ml, and by plotting K_{av} versus $\lg(M_r)$, K_{av} versus M_r and $\lg(M_r)$ versus V_e calibration curves were calculated with linear interpolation. The mean apparent molecular weight corresponding to each fraction number was then determined by averaging all three calculated values.

The buffer used for gel filtration contained 10 mM KCl, 1 mM EDTA, 1 mM EGTA, 1 mM $MgCl_2$ and 20 mM HEPES (pH 7.5 KOH); 135 mM KCl for ribosomes.

Detection of intracellular potassium concentration

HeLa cells were grown in 96-well plates until 80–90% confluency. The cells were treated with α-toxin (300 ng/ml) and with nigericin (10 μM) as positive control. PBFI (potassium binding benzofuran isophthalate; Invitrogen) was added to the cells 1 or 5 h later and incubated for 1 h at 37 °C, 5% CO_2. The samples were measured with fluorescent plate reader (Victor3, Perkin Elmer; excitation: 340 nm, emission: 515 nm).

Statisitical analysis

Student's *t*-test was routinely performed to test for statistical significance of the results ($*P<0.05$, $**P<0.01$, $***P<0.005$). The sample size (number of experiments) has always been indicated in the figure as ($n = x$).

Supplementary data

Supplementary data are available at *The EMBO Journal* Online (http://www.embojournal.org).

Acknowledgements

We thank Heiko Mühl for providing human keratinocytes, Andreas Villunger for kindly providing caspase-2- and PIDD-deficient MEFs, Dr Nika Danial for BAX/BAK DKO MEFs, Prof. Richard Flavell for Caspase-3/7 double-deficient MEFs, Florian Buhr for providing ribosomes for calibrating gel filtration columns. We also thank Kristina Wagner and Carrie Anderson for excellent technical assistance. We are grateful to Dorothea Imre-Fecske for art work presented in 7 H. This work is partially supported by an Emmy Noether programme grant RA1739/1-1 to KR from the DFG, and partially by SFB-TR34 from the DFG to BS, and VD acknowledges support from CEF-MC. MH acknowledges support from DFG (SFB 490; project D3).

Author contributions: GI performed most of the experiments, analysed and interpreted data and prepared figures. A-NT performed supporting experiments. DMzH contributed to microscopy analysis. BS, MH, GvdG and DRG contributed valuable materials and inputs into the study. BT contributed to mass spectrometric analysis. JH and VD contributed to gel filtration studies and data analysis interpretation. KR conceived and designed the project, analysed and interpreted data, co-ordinated the study and wrote the paper with inputs from all authors.

Conflict of interest

The authors declare that they have no conflict of interest.

References

Abrami L, Fivaz M, Glauser PE, Sugimoto N, Zurzolo C & van der Goot FG (2003) Sensitivity of polarized epithelial cells to the pore-forming toxin aerolysin. *Infect Immun* **71:** 739–746

Abrami L, Fivaz M, van der Goot FG (2000) Adventures of a pore-forming toxin at the target cell surface. *Trends Microbiol* **8:** 168–172

Baliga BC, Read SH, Kumar S (2004) The biochemical mechanism of caspase-2 activation. *Cell Death Differ* **11:** 1234–1241

Bantel H, Sinha B, Domschke W, Peters G, Schulze-Osthoff K, Janicke RU (2001) Alpha-toxin is a mediator of Staphylococcus aureus-induced cell death and activates caspases via the intrinsic death pathway independently of death receptor signaling. *J Cell Biol* **155:** 637–648

Bhakdi S, Tranum-Jensen J (1991) Alpha-toxin of Staphylococcus aureus. *Microbiol Rev* **55:** 733–751

Bischofberger M, Gonzalez MR, van der Goot FG (2009) Membrane injury by pore-forming proteins. *Curr Opin Cell Biol* **21:** 589–595

Bouchier-Hayes L, Oberst A, McStay GP, Connell S, Tait SW, Dillon CP, Flanagan JM, Beere HM, Green DR (2009) Characterization of cytoplasmic caspase-2 activation by induced proximity. *Mol Cell* **35:** 830–840

Chen F, He Y (2009) Caspase-2 mediated apoptotic and necrotic murine macrophage cell death induced by rough *Brucella abortus*. *PLoS One* **4:** e6830

Craven RR, Gao X, Allen IC, Gris D, Bubeck WJ, Elvania-Tekippe E, Ting JP, Duncan JA (2009) *Staphylococcus aureus* alpha-hemolysin activates the NLRP3-inflammasome in human and mouse monocytic cells. *PLoS One* **4:** e7446

Draeger A, Monastyrskaya K, Babiychuk EB (2011) Plasma membrane repair and cellular damage control: the annexin survival kit. *Biochem Pharmacol* **81:** 703–712

Fernandes-Alnemri T, Wu J, Yu JW, Datta P, Miller B, Jankowski W, Rosenberg S, Zhang J, Alnemri ES (2007) The pyroptosome: a supramolecular assembly of ASC dimers mediating inflammatory cell death via caspase-1 activation. *Cell Death Differ* **14:** 1590–1604

Galdiero S, Gouaux E (2004) High resolution crystallographic studies of alpha-hemolysin-phospholipid complexes define heptamer-lipid head group interactions: implication for understanding protein-lipid interactions. *Protein Sci* **13:** 1503–1511

Genestier AL, Michallet MC, Prevost G, Bellot G, Chalabreysse L, Peyrol S, Thivolet F, Etienne J, Lina G, Vallette FM, Vandenesch F, Genestier L (2005) *Staphylococcus aureus* Panton-Valentine leukocidin directly targets mitochondria and induces Bax-independent apoptosis of human neutrophils. *J Clin Invest* **115:** 3117–3127

Gong J, Traganos F, Darzynkiewicz Z (1994) A selective procedure for DNA extraction from apoptotic cells applicable for gel electrophoresis and flow cytometry. *Anal Biochem* **218:** 314–319

Gonzalez MR, Bischofberger M, Freche B, Ho S, Parton RG, van der Goot FG (2011) Pore-forming toxins induce multiple cellular responses promoting survival. *Cell Microbiol* **13:** 1026–1043

Gonzalez MR, Bischofberger M, Pernot L, van der Goot FG, Freche B (2008) Bacterial pore-forming toxins: the (w)hole story? *Cell Mol Life Sci* **65:** 493–507

Gurcel L, Abrami L, Girardin S, Tschopp J, van der Goot FG (2006) Caspase-1 activation of lipid metabolic pathways in response to bacterial pore-forming toxins promotes cell survival. *Cell* **126:** 1135–1145

Haslinger B, Strangfeld K, Peters G, Schulze-Osthoff K, Sinha B (2003) *Staphylococcus aureus* alpha-toxin induces apoptosis in peripheral blood mononuclear cells: role of endogenous tumour necrosis factor-alpha and the mitochondrial death pathway. *Cell Microbiol* **5:** 729–741

Husmann M, Beckmann E, Boller K, Kloft N, Tenzer S, Bobkiewicz W, Neukirch C, Bayley H, Bhakdi S (2009) Elimination of a bacterial pore-forming toxin by sequential endocytosis and exocytosis. *FEBS Lett* **583:** 337–344

Iacovache I, Bischofberger M, van der Goot FG (2010) Structure and assembly of pore-forming proteins. *Curr Opin Struct Biol* **20:** 241–246

Jesenberger V, Procyk KJ, Yuan J, Reipert S, Baccarini M (2000) Salmonella-induced caspase-2 activation in macrophages: a novel mechanism in pathogen-mediated apoptosis. *J Exp Med* **192:** 1035–1046

Kroemer G, Galluzzi L, Vandenabeele P, Abrams J, Alnemri ES, Baehrecke EH, Blagosklonny MV, El-Deiry WS, Golstein P, Green DR, Hengartner M, Knight RA, Kumar S, Lipton SA, Malorni W, Nunez G, Peter ME, Tschopp J, Yuan J, Piacentini M *et al* (2009) Classification of cell death: recommendations of the Nomenclature Committee on Cell Death 2009. *Cell Death Differ* **16:** 3–11

Krumschnabel G, Sohm B, Bock F, Manzl C, Villunger A (2009) The enigma of caspase-2: the laymen's view. *Cell Death Differ* **16:** 195–207

Lamkanfi M, Dixit VM (2010) Manipulation of host cell death pathways during microbial infections. *Cell Host Microbe* **8:** 44–54

Lavrik IN, Golks A, Baumann S, Krammer PH (2006) Caspase-2 is activated at the CD95 death-inducing signaling complex in the course of CD95-induced apoptosis. *Blood* **108:** 559–565

Mace PD, Riedl SJ (2010) Molecular cell death platforms and assemblies. *Curr Opin Cell Biol* **22:** 828–836

Manzl C, Krumschnabel G, Bock F, Sohm B, Labi V, Baumgartner F, Logette E, Tschopp J, Villunger A (2009) Caspase-2 activation in the absence of PIDDosome formation. *J Cell Biol* **185:** 291–303

McStay GP, Salvesen GS, Green DR (2008) Overlapping cleavage motif selectivity of caspases: implications for analysis of apoptotic pathways. *Cell Death Differ* **15:** 322–331

Meier P, Vousden KH (2007) Lucifer's labyrinth—ten years of path finding in cell death. *Mol Cell* **28:** 746–754

Nutt LK, Buchakjian MR, Gan E, Darbandi R, Yoon SY, Wu JQ, Miyamoto YJ, Gibbons JA, Andersen JL, Freel CD, Tang W, He C, Kurokawa M, Wang Y, Margolis SS, Fissore RA, Kornbluth S (2009) Metabolic control of oocyte apoptosis mediated by 14-3-3zeta-regulated dephosphorylation of caspase-2. *Dev Cell* **16:** 856–866

Nutt LK, Margolis SS, Jensen M, Herman CE, Dunphy WG, Rathmell JC, Kornbluth S (2005) Metabolic regulation of oocyte cell death through the CaMKII-mediated phosphorylation of caspase-2. *Cell* **123:** 89–103

Read SH, Baliga BC, Ekert PG, Vaux DL, Kumar S (2002) A novel Apaf-1-independent putative caspase-2 activation complex. *J Cell Biol* **159:** 739–745

Rudel T, Kepp O, Kozjak-Pavlovic V (2010) Interactions between bacterial pathogens and mitochondrial cell death pathways. *Nat Rev Microbiol* **8:** 693–705

Saleh M, Green DR (2007) Caspase-1 inflammasomes: choosing between death and taxis. *Cell Death Differ* **14:** 1559–1560

Shi Y (2004) Caspase activation: revisiting the induced proximity model. *Cell* **117:** 855–858

Srivastava SS, Pany S, Sneh A, Ahmed N, Rahman A, Musti KV (2009) Membrane bound monomer of Staphylococcal alpha-hemolysin induces caspase activation and apoptotic cell death despite initiation of membrane repair pathway. *PLoS One* **4:** e6293

Thompson GJ, Langlais C, Cain K, Conley EC, Cohen GM (2001) Elevated extracellular [K+] inhibits death-receptor- and chemical-mediated apoptosis prior to caspase activation and cytochrome c release. *Biochem J* **357:** 137–145

Thornberry NA, Lazebnik Y (1998) Caspases—enemies within. *Science* **281:** 1312–1316

Tinel A, Tschopp J (2004) The PIDDosome, a protein complex implicated in activation of caspase-2 in response to genotoxic stress. *Science* **304:** 843–846

Troy CM, Shelanski ML (2003) Caspase-2 redux. *Cell Death Differ* **10:** 101–107

Tu S, McStay GP, Boucher LM, Mak T, Beere HM, Green DR (2006) *In situ* trapping of activated initiator caspases reveals a role for caspase-2 in heat shock-induced apoptosis. *Nat Cell Biol* **8:** 72–77

Walev I, Martin E, Jonas D, Mohamadzadeh M, Muller-Klieser W, Kunz L, Bhakdi S (1993) Staphylococcal alpha-toxin kills human keratinocytes by permeabilizing the plasma membrane for monovalent ions. *Infect Immun* **61:** 4972–4979

Walev I, Reske K, Palmer M, Valeva A, Bhakdi S (1995) Potassium-inhibited processing of IL-1 beta in human monocytes. *EMBO J* **14:** 1607–1614

Warny M, Kelly CP (1999) Monocytic cell necrosis is mediated by potassium depletion and caspase-like proteases. *Am J Physiol* **276:** C717–C724

Wilke GA, Bubeck WJ (2010) Role of a disintegrin and metalloprotease 10 in *Staphylococcus aureus* alpha-hemolysin-mediated cellular injury. *Proc Natl Acad Sci USA* **107:** 13473–13478

